Pharmacological disruption of the Notch transcription factor complex

Lehal, Rajwinder ; Zaric, Jelena ; Vigolo, Michele ; Urech, Charlotte ; Frismantas, Viktoras ; Zangger, Nadine ; Cao, Linlin ; Berger, Adeline ; Chicote, Irene ; Loubéry, Sylvain ; Choi, Sung Hee ; Koch, Ute ; Blacklow, Stephen C ; Palmer, Hector G ; Bornhauser, Beat ; González-Gaitán, Marcos ; Arsenijevic, Yvan ; Zoete, Vincent ; Aster, Jon C ; Bourquin, Jean-Pierre ; Radtke, Freddy

Abstract: Notch pathway signaling is implicated in several human cancers. Aberrant activation and mutations of Notch signaling components are linked to tumor initiation, maintenance, and resistance to cancer therapy. Several strategies, such as monoclonal antibodies against Notch ligands and receptors, as well as small-molecule -secretase inhibitors (GSIs), have been developed to interfere with Notch receptor activation at proximal points in the pathway. However, the use of drug-like small molecules to target the downstream mediators of Notch signaling, the Notch transcription activation complex, remains largely unexplored. Here, we report the discovery of an orally active small-molecule inhibitor (termed CB-103) of the Notch transcription activation complex. We show that CB-103 inhibits Notch signaling in primary human T cell acute lymphoblastic leukemia and other Notch-dependent human tumor cell lines, and concomitantly induces cell cycle arrest and apoptosis, thereby impairing proliferation, including in GSI-resistant human tumor cell lines with chromosomal translocations and rearrangements in Notch genes. CB-103 produces Notch loss-of-function phenotypes in flies and mice and inhibits the growth of human breast cancer and leukemia xenografts, notably without causing the dose-limiting intestinal toxicity associated with other Notch inhibitors. Thus, we describe a pharmacological strategy that interferes with Notch signaling by disrupting the Notch transcription complex and shows therapeutic potential for treating Notch-driven cancers.

DOI: https://doi.org/10.1073/pnas.1922606117

Biological Sciences

Applied Biological Sciences
Medical Sciences

Pharmacological disruption of the Notch transcription factor complex

Rajwinder Lehal[1,2], Jelena Zaric[1], Michele Vigolo[1,2], Charlotte Urech[2], Viktoras Frismanatas[3,4], Nadine Zangger[5], Linlin Cao[1], Adeline Berger[6], Irene Chicote [7,] Sylvain Loubéry[8], Sung Hee Choi[9], Ute Koch[1], Stephen C. Blacklow[9], Hector G. Palmer[7], Beat Bornhauser[3,4], Marcos Gonzalez-Gaitan[8], Yvan Arsenijevic[6], Vincent Zoete[5, 10], Jon C. Aster[11], Jean-Pierre Bourquin[3,4], and Freddy Radtke[1*]

[1]Swiss Institute for Experimental Cancer Research (ISREC), Ecole Polytechnique Fédérale de Lausanne (EPFL), 1015 Lausanne, Switzerland.
[2]Cellestia Biotech SA, Hochbergerstasse 60C, 4057, Basel, Switzerland
[3]Department of Oncology, University Children's Hospital Zürich, Zürich, Switzerland
[4]Children's Research Center, University Children's Hospital Zürich, Zürich, Switzerland;
[5]Bioinformatics Core Facility, Swiss Institute of Bioinformatics (SIB), Lausanne 1015, Switzerland
[6] Unit of Gene Therapy and Stem Cell Biology, Department of Ophtalmology, Jules-Gonin Eye Hospital, University of Lausanne, Lausanne, Switzerland.
[7]Stem Cells and Cancer Group, Vall d'Hebron Institute of Oncology, Barcelona, Spain.
[8]Department of Biochemistry, Faculty of Sciences, University of Geneva, Quai Ernest Ansermet 30, 1211 Geneva, Switzerland
[9]Department of Biological Chemistry and Molecular Pharmacology, Blavatnik Institute, Harvard Medical School, Boston, MA 02115, USA.
[10]Computer-Aided Molecular Engineering, Department of Oncology, Ludwig Institute for Cancer Research, University of Lausanne, Lausanne, Switzerland
[11]Department of Pathology, Brigham and Women's Hospital, and Harvard Medical School, Boston, MA 02115, USA.

Corresponding author: Freddy.Radtke@epfl.ch

Keywords: Notch, small molecule inhibitor, Cancer

Abstract

Notch pathway signaling is implicated in several human cancers. Aberrant activation and mutations of Notch signaling components are linked to tumor initiation, maintenance and resistance to cancer therapy. Several strategies, such as monoclonal antibodies (MAbs) against Notch ligands and receptors, as well as small molecule γ-secretase inhibitors (GSIs), have been developed to interfere with Notch receptor activation at proximal points in the pathway. However, the use of drug-like small molecules to target the downstream mediators of Notch signaling, the Notch transcription activation complex, remains largely unexplored. Here, we report the discovery of an orally active small molecule inhibitor (termed CB-103) of the Notch transcription activation complex. We show that CB-103 inhibits Notch signaling in primary human T-ALL and other Notch-dependent human tumor cell lines, and concomitantly induces cell cycle arrest and apoptosis, thereby impairing proliferation, including in GSI-resistant human tumor cell lines with chromosomal translocations and rearrangements in Notch genes. CB-103 produces Notch loss-of-function phenotypes in flies and mice and inhibits the growth of human breast cancer and leukemia xenografts, notably without causing the dose-limiting intestinal toxicity associated with other Notch inhibitors. Thus, we describe a pharmacological strategy that interferes with Notch signaling by disrupting the Notch transcription complex and shows therapeutic potential for treating Notch-driven cancers.

Significance statement

The Notch signaling cascade is deregulated by oncogenic lesions in human cancers and has therefore become an attractive therapeutic target. Inhibitory monoclonal antibodies and small molecule γ-secretase inhibitors have been developed to target the pathway at the most proximal point of the cascade. Major hurdles to the therapeutic application of these Notch inhibitors have been prevalent dose limiting toxicities in the intestine. Here we report identification and preclinical validation of a small molecule (CB-103) that inhibits the pathway at the level of Notch transcription complex without causing intestinal toxicity. Its properties and mechanism of action provide CB-103 with a more favorable therapeutic index than other types of Notch targeting agents, a feature that is currently being tested in cancer patients.

Introduction

Transcription factors (TF) are key mediators of cellular processes and cell states. In cancer, TFs are commonly deregulated indirectly by aberrant upstream signaling cascades or directly by pathogenic mutations and or translocations. Although in principle an attractive class of therapeutic targets, TFs are largely considered undruggable due to the absence of surface pockets amenable to effective targeting with small molecules. Thus, most currently available targeted cancer therapeutics aim at inhibiting oncogenic signaling pathways at the most proximal part of the cascade, either through antibodies against ligands or surface receptors, or using small molecules that inhibit the enzymatic activities of receptor-associated kinases.

The Notch signaling cascade is one example of a pathway that has emerged as a rational therapeutic target in several cancers. In the adult, Notch signaling in progenitor and stem

cells regulates tissue homeostasis, self-renewal, and differentiation in several organs and cell types, including the intestine, vasculature, and hematopoietic system(1).

Notch signaling is initiated through the interaction of a receptor and ligand on neighboring cells. This event results in sequential proteolytic cleavages of the receptor mediated by metalloproteases of the ADAM family and the γ-secretase multiprotein complex that liberate the Notch intracellular domain (NICD). NICD subsequently traffics to the nucleus, binds the TF RBPJ, and recruits other coactivators such as mastermind proteins (MAML1-3) and p300, forming a transcription activation complex that initiates the expression of downstream target genes(2).

Next-generation sequencing of cancer genomes has identified numerous oncogenic gain-of-function mutations in *NOTCH1* or *NOTCH2* in B and T cell leukemias and lymphomas(3–5) and solid cancers such as adenoid cystic carcinoma(6) and breast carcinoma(7, 8). These mutated or truncated genes encode proteins that are processed to NICD constitutively and/or have increased stability in their active forms, increasing the expression of target genes that deregulate cell growth and survival. Several strategies, such as MAbs against Notch ligands(9–11) and receptors(12, 13), and small molecule GSIs(14, 15), have been developed to block Notch receptor activation at proximal points in the pathway. Whereas MAbs have the advantage of specifically inhibiting individual ligands or receptors, GSIs are pan-Notch inhibitors that block signaling through all 4 Notch receptors(16). GSIs were originally developed for treating Alzheimer disease because they inhibit the cleavage of amyloid precursor protein (APP). In addition, they also block the proteolytic cleavage step (S3 cleavage) that generates NICD, leading to their widespread experimental use as Notch inhibitors(1, 14). However, GSIs also block the processing of more than 90 other substrates, which may complicate the interpretation of results produced by GSIs(16). Although both MAbs and GSIs have shown beneficial effects in preclinical Notch-driven tumor models and clinical studies (12, 17–21), none of these Notch inhibitors have been clinically approved, largely due to on-target dose-limiting toxicities of the intestinal

epithelium(22, 23). Treatment of patients with GSI is frequently associated with diarrhea, vomiting, and nausea, which may be severe(24, 25). To avoid this toxicity, clinical trials in Notch- driven cancers have relied on intermitting dosing of GSIs(14). However, the question remains whether intermittent dosing strategies sustain Notch inhibition long enough to achieve therapeutic efficacy.

There have also been attempts to target the pathway downstream of the γ-secretase mediated activation of Notch receptors. One is based on the finding that truncated forms of MAML1 that bind RBPJ-NICD complex but lack the ability to recruit other co-activators function in a dominant negative manner(26–28). Based on this concept, Bradner and colleagues synthesized a stapled peptide named SAHM1 (stapled α-helical peptide derived from MAML1) designed to mimic dominant negative forms of MAML1(29). However, developing drug-like stapled peptides as therapeutics remains challenging due to manufacturing, stability and pharmacokinetic issues. Another approach utilized screens to identify the small molecule Mastermind recruitment-1 (IMR-1), which is also proposed to have dominant-negative MAML-like activity(30). Finally, a recent report describes the identification of a small molecule that blocks the interaction between RBPJ and SHARP, a protein that forms a corepressor complex with RBPJ(31). However, this approach does not inhibit NOTCH signaling, but rather leads to de-repression of NOTCH target genes (31). Although all of these Notch TF complex-modulating compounds show inhibitory activities in cellular assays, it remains to be determined whether these inhibitors possess drug-like properties, as none of these compounds have been tested in clinical trials.

Here, we report the discovery and preclinical validation of a novel, orally active small molecule (termed CB-103) that interferes with the function of the Notch transcription complex. CB-103 induces loss-of-function phenotypes in flies and mice and has antitumor activity in xenograft models of Notch addicted human leukemia and carcinoma without causing gut toxicity.

CB-103 possesses excellent drug-like properties and is currently being evaluated in a phase-I clinical trial in cancer patients.

Results

Identification of CB-103 as a Notch inhibitor

Seeking to discover small molecule inhibitors of Notch signaling, we developed a cell-based co-culture assay amenable to high-throughput screening of chemical compound libraries. This screen utilized a co-culture system consisting of 'signal receiving' HeLa cells expressing Notch1 in combination with a Notch responsive luciferase reporter, and 'signal sending' HeLa cells expressing the Notch ligand Delta-like 4 (DL4) (**Figs. 1*A* and *B***).

A screen of 67,253 compounds from commercially available libraries identified 341 compounds with Notch inhibitory activity. Computer-aided self-organizing mapping programs that cluster compounds based on structural similarities allowed reduction of the number of hits to 98, of which 33 were validated by a secondary screen in the same co-culture assay. These compounds were then assayed for their ability to block signaling driven by a dominant active form of the Notch1 receptor (N1-ICD) (**Fig. 1*C***). Importantly, this approach enables identification of compounds that act downstream of the γ-secretase mediated S3 cleavage event. Employing this strategy we identified the compound 6-(4-(*tert*-butyl)phenoxy)pyridin-3-amine, hereafter named CB-103 (**Fig. 1*D***). To assess whether CB-103 specifically inhibits Notch1 or is also active against other Notch receptors, we tested the ability of CB-103 to inhibit Notch2-, Notch3-and Notch4-mediated signaling using the *in vitro* co-culture assay. CB-103 inhibited Notch signaling mediated by each of the receptors tested in a dose dependent manner (**Figs. 1*E and F***). As was observed for N1-ICD (**Fig. 1*G***), CB-103 was also able to block the activity of the dominant-active forms of Notch2, Notch3 and Notch4 (N2-ICD, N3-ICD and N4-ICD respectively) (**Fig. 1*H***). Overall, CB-103

inhibited both ligand dependent and ligand independent Notch activation in cell-based assays, with IC_{50} values ranging from 0.9-3.9 μM (**Figs.1 *F* and *H***); CB-103 did not inhibit Wnt or Hedgehog signaling using reporter assays (*SI Appendix,* Fig. S1A and B).

In light of the above data, we hypothesized that CB-103 acts to prevent Notch-mediated transcription and thus sought to substantiate this prediction. Experiments using a N1-ICD-GFP fusion protein indicated that CB-103 does not prevent nuclear translocation of N1-ICD (**Fig. 1*I***), excluding impaired trafficking as a mechanism of action. An alternative possibility is that it interferes with a functional assembly of the transcription complex. Consistent with this, expression of increasing amounts of the co-factor MAML1 counteracted the inhibitory effect of CB-103 (**Fig. 1*J***), suggesting that CB-103 impairs the recruitment and/or assembly of components of the Notch transcription complex.

CB-103 inhibits growth of Notch addicted human T-ALL cell lines through modulation of the Notch transcription complex.

To further establish CB-103 as a *bona fide* Notch inhibitor, we tested its ability to directly inhibit the growth of Notch-dependent cancer cells by initially focusing on T-cell acute lymphoblastic leukemia (T-ALL). More than 50% of T-ALL patients harbor activating *NOTCH1* mutations resulting in increased Notch signaling(3). Treatment of the *NOTCH1*-mutated human T-ALL cell line RPMI-8402 and the NOTCH3-driven human TALL-1 cell line with CB-103 or a GSI resulted in down regulation of the Notch target genes *HES1*, *MYC* and *DTX1* (*SI Appendix,* Fig. S2A and B), as well as down-regulation of *NOTCH1* (*SI Appendix*, Fig. S2 C). Interestingly, protein levels of N1-ICD were unaffected by short-term (6 hour) treatment with CB-103 (*SI Appendix*, Fig. S2C), but were significantly reduced at later time points (24 and 48 hours) (*SI Appendix*, Fig. S2D and E). In contrast, protein levels of RBPJ were unaffected (*SI Appendix,* Fig. S2 E). Simultaneous treatment of RPMI-8402

cells with CB-103 and a proteasome inhibitor did not restore N1-ICD levels, suggesting that CB-103 does not impact N1-ICD protein levels by enhancing proteasomal degradation (*SI Appendix,* Fig. S2 F). As NOTCH1 exhibits positive autoregulation in T-ALL cells, these results are consistent with a fall in N1-ICD levels due to inhibition of *NOTCH1* transcription. In addition, CB-103 induced profound cell growth inhibition in both RPMI-8402 and T-ALL1 cells (*SI Appendix,* Fig. S2G-H). In contrast, growth of the Notch-independent HeLa cell line was unaffected by either CB-103 or GSI treatment (*SI Appendix,* Fig. S2I). Global gene expression analysis of CB-103-treated *NOTCH1*-mutated T-ALL cell lines KOPT-K1 and HBP-ALL further confirmed down regulation of N1-ICD-driven growth-promoting genes, including *MYC*, the main oncogenic driver directly regulated by Notch in T-ALL(32, 33) (*SI Appendix,* Fig. S3A and B).

To gain insight into the molecular mechanism underlying CB-103 inhibition of Notch-mediated transcription, we generated RPMI-8402 T-ALL cell lines with reduced sensitivity to CB-103 and then investigated a possible mechanism of insensitivity – mutation - by exome sequencing, motivated by the hypothesis that drug insensitivity could occur through gene mutations affecting the drug's target(s)(34). Exome sequencing of CB-103 insensitive RPMI-8402 T-ALL cells identified a G193R mutation within the BTD domain of RBPJ. Importantly, engineered expression of a *V5-tagged RBPJ*^{G193R} mutant gene in parental RPMI-8402 cells shifted the IC_{50} for CB-103 from 2.6 μM to >100 μM, whereas expression of *V5-tagged WT RBPJ* had minimal effects, indicating that this specific single amino acid change is sufficient to confer insensitivity to CB-103 treatment (**Figs. 2*A-C***).

Next, we performed computational docking studies. CB-103 was docked on the full NOTCH1 transcription complex / HES1 promoter DNA system to determine a possible binding mode on the native structure(35). Among the calculated binding modes, one confirmed the BTD domain of RBPJ as possible binding site for CB-103 and identified

several key RBPJ amino acid residues **(Fig. 2*A*)**. Expression of engineered forms of RBPJ bearing mutations in these residues, specifically V5-tagged RBPJ^{F196A}, V5-tagged RBPJ^{L245A} or V5-tagged RBPJ^{L248A}, but a control mutant, V5-tagged RBPJ^{G194R}, in parental RPMI-8402 cells conferred resistance to CB-103 (**Figs. 2*B* and *C* and** *SI Appendix,* Fig. S4). Thus, combined docking and mutational analysis support the binding of CB-103 to this pocket in the BTD domain. Notably, this pocket is also important for binding of the N1-ICD RAM domain to CSL, providing an explanation for how CB-103 impairs the formation and activity of the Notch1 transcription complex.

In further support of this model, CB-103 also interfered with recovery of N1-ICD in immunoprecipitates prepared from RPMI-8402 cells expressing V5-WT-RBPJ, but not from cells expressing V5-RBP-J^{G193R} protein (**Figs. 3*A* and B**). Furthermore, CB-103 reduced the occupancy of RBPJ and N1-ICD on genomic Notch-response elements associated with the Notch target genes *HES1*, *DTX1*, and *MYC* in RPMI-8402 cells expressing V5-WT-RBPJ but not in cells expressing the V5-RBP-J^{G193R} mutant (**Fig. 3C**). Taken together, these results strongly suggest that CB-103 inhibits Notch mediated transcription by interfering with assembly of the Notch1 transcription complex.

The majority of Notch/RBPJ binding sites that mediate acute changes in gene expression are found in enhancers(36). These genomic response elements are of two distinct types, one containing monomeric RBPJ sites and the second dimeric head-to-head RBPJ sites separated by 15-17 base pairs, an element called a sequence-pair site (SPS) that supports loading of dimeric Notch TF complexes. SPS-mediated Notch signaling is important for T cell maturation and leukemic transformation but dispensable for T cell fate specification in mice (37, 38). To determine whether CB-103 preferentially inhibited elements containing SPSs versus head-to-tail oriented RBPJ binding sites, we performed luciferase reporter gene assays. Although SPSs-driven reporters elicited a much stronger signal compared to head-to-

tail oriented RBPJ-driven promoters, both were equally sensitive to CB-103. Thus, CB-103 inhibits both monomeric and dimeric Notch1 TF complexes, which agrees with the proposed mode of action of CB-103 (*SI Appendix,* Fig. S5).

Next, we performed kinetic gene expression analysis using SLAM-seq on vehicle and CB-103 treated RPMI-8402 T-ALL cells to investigate potential differences in the CB-103 sensitivity of promoter- and enhancer-driven Notch target genes. Pathway analysis from the Hallmark collection revealed E2F targets, MYC targets, and PI3K AKT MTOR signaling as being the most rapidly downregulated pathways. Interestingly, the Notch target genes *DTX1*, *HES1*, *NOTCH3* and *NOTCH1*, which are regulated by response elements found in promoters or intragenic enhancers, were downregulated faster than target genes that are regulated by long distance enhancers, such as *MYC, GIMAP1, 5, 6* and *8*, suggesting that different Notch target genes may have varying sensitivities and or kinetics of response to CB-103 (*SI Appendix,* Fig. S6).

In previous studies, the stapled peptide and small molecules SAHM1 and IMR-1 were also claimed to target the Notch transcription complex(29, 30), and we therefore compared their activities with CB-103 in reporter gene assays and in Notch-driven T-ALL cells. The activity of SAHM1 in reporter gene assays was indistinguishable from unstapled control peptide, and although SAHM1 was cytotoxic, unlike CB-103, it did not downregulate *MYC* expression in RPMI-8402 T-ALL cells (*SI Appendix,* Fig. S7). In the same assays, we failed to identify any effect of IMR-1 on *MYC* levels, or RPMI-8402 cell growth at doses up to 10 μM (*SI Appendix,* Fig. S7). Thus, CB-103 acts by a markedly different mechanism than SAHM1 and IMR-1 with respect to the expected activities of direct Notch transcription complex.

CB-103 function *in vivo* recapitulates genetic Notch loss-of-function phenotypes without causing gut toxicity.

Prior to investigating the *in vivo* activity of CB-103, we profiled the compound to determine its drug-like and ADME/PK (absorption, distribution, metabolism, excretion and pharmacokinetic) properties (*SI Appendix,* Fig. S8). Then we assessed CB-103's ability to affect a variety of Notch-dependent cellular processes. First, we studied the effect of CB-103 on the development of mechanosensory organs in *Drosophila*, which consist of four distinct lineages (socket, shaft, sheath and neuron) derived from a single sensory organ precursor cell (39). Notch signaling loss induces aberrant sensory organ lineages, including lineages composed of two neurons and no sheath cells, indicative of sheath-to-neuron transformation(39). Treatment of developing sensory organs with CB-103 resulted in increased numbers of neurons, similar to the effect produced by GSI (DAPT), demonstrating that CB-103 inhibits Notch-dependent cell fate specification in flies (*SI Appendix,* Fig. S9).

We extended these findings to mammals and investigated how CB-103 affects five Notch-dependent phenotypes in mice: i) development of splenic marginal zone B (MZB) cells; ii) thymic T cell development; iii) generation of $Esam^{+}$ dendritic cells; iv) sprouting of endothelial cells; and v) induction of goblet cell differentiation in the small intestine. Each of these processes strictly require Notch signaling (40–46). As expected, treatment with CB-103 (*SI Appendix,* Fig. S10A) resulted in a dramatic, reversible reduction of $B220^{+}CD21^{hi}CD23^{int}$ MZB cells (*SI Appendix,* Fig. S10B), mimicking phenotypes caused by loss of *Notch2*(38) or *Dll1*(39). Osmotic pump-mediated delivery to maintain sustained exposure to CB-103 resulted in a concentration-dependent reduction of MZB cells and revealed that a level of 700 ng/ml (2.8 μM) in plasma is sufficient to inhibit Notch signaling **(***SI Appendix,* Fig. S10C and D**).** Similarly, we observed impaired thymic T cell development **(***SI Appendix,* Fig. S11A**)**, reduced numbers of $Esam^{+}CD11c^{+}CD8^{-}$ dendritic cells **(***SI Appendix,* Fig. S11B**)**, and

increased endothelial cell sprouting in CB-103 treated wild type mice (*SI Appendix,* Fig. S12).

In notable contrast, CB-103 treatment did not produce the expected intestinal phenotype. Genetic deletion of genes encoding *Notch1* and *Notch2* receptors or *Dll1* and *Dll4* ligands or *RBPJ*, as well as sustained treatment with potent GSIs, result in goblet cell metaplasia and reduced proliferation of crypt progenitor cells(40, 41, 47). Goblet cell metaplasia-associated intestinal toxicity is one of the main dose-limiting 'adverse events' in clinical trials using Notch targeting agents such as GSI or antagonistic Notch receptor antibodies(1). We treated mice with vehicle control, CB-103 or the GSI LY3039478. Mice treated with vehicle control or CB-103 were analyzed after one week and 4 weeks of treatment, while mice treated with LY3039478 were analyzed after one week due to treatment-related morbidity. Alcian blue and Ki67 staining revealed a dramatic increase in goblet cell numbers and a highly significant reduction in crypt cell proliferation in LY3039478 treated animals. In contrast, CB-103 treated animals showed only a moderate increase in goblet cell numbers and a moderate reduction in Ki67-positive crypt cells (**Figs. 4*A* and *B***).

To investigate the basis of the milder gut phenotype in CB-103-treated mice, we studied its effects on key downstream target genes. In the small intestine, Notch signaling directly regulates the expression of the stem cell marker gene *Olmf4* and members of the *Hes* family of TFs, which repress the transcriptional master regulator for secretory cells, Atoh1(48–50). *In situ* hybridization studies revealed that the expression of *Olmf4* and *Hes1* was nearly completely abrogated by CB-103 and LY3039478, thereby demonstrating Notch inhibitory activity of these agents in the gut. By contrast, LY3039478 treated animals had significantly higher levels of *Atoh1* transcripts compared to vehicle and CB-103 treated animals, which showed only a small increase in *Atoh1* transcripts relative to vehicle treated

animals (**Fig. 4*B***). To exclude possible confounding influences of variation in absorption or pharmacokinetic properties *in vivo*, we tested these compounds in intestinal organoid cultures created from wild type mice. LY3039478-treated organoids had a very different morphology than CB-103 treated cultures and showed increased goblet cell differentiation and decreased proliferation compared to vehicle or CB-103 treated organoids (*SI Appendix,* Fig. S13A). We again observed strong inhibition of the Notch pathway, as indicated by downregulation of direct Notch target genes *Olmf4, Hes1, Hes3* and *Hes5* to a similar degree by both CB-103 and LY3039478, whereas *Atoh1* transcripts were upregulated to higher levels in LY3039478 treated organoids (*SI Appendix,* Fig. S13B). These results show that while both compounds block Notch signaling in the intestine *in vivo* and in intestinal organoids, goblet cell metaplasia and profound growth inhibition were only observed with LY3039478 treatment, presumably due to the higher expression levels of *Atoh1*.

CB-103 blocks tumor growth of GSI-resistant cancers.

A potential advantage of a small molecule inhibitor of the Notch TF complex is the ability to block Notch signaling in tumors that are resistant to Notch-directed MAbs or GSIs by virtue of Notch gene rearrangements that lead to γ-secretase independent Notch activation. As a proof of principle, we studied via lentiviral expression of constitutively nuclear N1-ICD whether CB-103 could inhibit growth of Notch-dependent human DND-41 T-ALL cells rendered resistant to agents (such as GSI) that act upstream of the Notch TF complex. As expected, parental DND-41 cells exhibited reduced growth inhibition and Notch signaling following treatment with either LY3039478 or CB-103, whereas only CB-103 elicited growth arrest in DND-41 cells expressing N1-ICD (*SI Appendix,* Fig. S14A). CB-103 sensitivity was in turn rescued by ectopic expression of *MYC* (*SI Appendix,* Fig. S14B), consistent with prior work implicating *MYC* as a key Notch target gene in T-ALL cells (51).

Next, we investigated the ability of CB-103 to inhibit growth of Notch-dependent cancers that are resistant to MAbs and/or GSI therapy. We focused on triple negative breast cancer (TNBC), since approximately 10% have rearrangements in *NOTCH1* and/or *NOTCH2* that lead to constitutive, ligand-independent Notch activation(7, 8). As predicted, growth of the GSI-resistant HCC1187 cell line carrying a *NOTCH2* rearrangement(7) was inhibited by CB-103 treatment but not by RO4929097, a GSI previously assessed in clinical phase I/II studies (8) (**Fig. 5*A***). We subsequently established a stable luciferase reporter line to determine the ability of CB-103 to inhibit growth of HCC1187 following xenotransplantation. CB-103 treated animals showed remarkable growth inhibition and reduced tumor burden compared to vehicle treated animals (**Fig. 5*B***). *CCDN1*, a known Notch target in breast cancer(52, 53), was downregulated in tumors from CB-103 treated animals compared to controls (**Fig. 5*C***). Moreover, CB-103 mediated tumor growth inhibition was accompanied by reduced Ki67 and increased Caspase 3 staining, while CD31 staining was similar in vehicle and CB-103 treated animals (and *SI Appendix,* Fig. S15). Our data provide proof-of-concept that CB-103 can inhibit growth of "Notch-addicted" cancer cells expressing mutated forms of Notch that cannot be targeted with agents that act upstream of the Notch TF complex. Furthermore, patient-derived xenotransplanation (PDX) experiments using a NOTCH1-positive oxaliplatin-resistant colorectal cancer sample(54) revealed that CB-103 resensitizes this tumor to oxaliplatin treatment *in vivo* (**Fig. 5*D***).

To extend these findings to primary human cancers, we investigated the ability of CB-103 to inhibit the growth of 19 primary T-ALLs, the human tumor with the highest frequency of Notch gain-of-function mutations, in a co-culture model(47). Dose response profiles indicated that CB-103 induced growth inhibition in ~50% of the cases tested with IC_{50} values in the sub-micromolar range (**Fig. 5*E***). Importantly, the ability of CB-103 to reduce tumor growth correlated strictly with Notch activation status, as only tumors containing N1-ICD

responded to CB-103 treatment. Furthermore, growth inhibition induced by CB-103 was associated with the presence of elevated levels of N1-ICD pre-treatment and decreased N1-ICD levels post-treatment, but did not strictly correlate with the mutation status of *NOTCH1*, or *FBXW7* (**Fig. 5*F***). These results indicate that CB-103 selectively inhibits the growth of T-ALLs with ongoing NOTCH1 activation and supports prior studies suggesting that the level of N1-ICD predicts tumor response to Notch pathway inhibitors(44). In line with these *ex-vivo* results, CB-103 prolonged the survival of mice bearing a *NOTCH1*-mutated T-ALL PDX model compared to vehicle treatment (**Fig. 5*G*, left panel**), an antitumor effect that was also associated with decreased N1-ICD levels (**Fig. 5*G*, right panels**). A second independent N1-ICD positive T-ALL PDX model also showed significantly reduced tumor burden in mice with either high or low tumor burden (>20% and <2% leukemic blasts in the peripheral blood) at treatment initiation, as indicated by percentages of circulating huCD45^{+}CD7^{+} T-ALL blasts after CB103 treatment **(Fig. 5*H*)**.

Discussion

In the last decade unbiased next generation sequencing efforts of human cancer specimens have identified activating genetic aberrations in NOTCH genes in a broad spectrum of cancers, including T-ALL, adenoid cystic carcinoma, chronic lymphocytic leukemia, marginal zone B cell lymphoma and breast cancer(3, 6, 7, 55). Moreover, many preclinical studies have implicated Notch signaling in almost all hallmarks of cancer, highlighting why this signaling pathway is an intriguing, but complex, therapeutic target(56).

Herein we describe a cell-based high throughput screen that led to the identification and characterization of novel small molecule inhibitor (CB-103) of the Notch cascade. CB-103 is a pan Notch inhibitor as it can block Notch-mediated signaling of all four Notch receptors (Fig.1), similar to GSIs. Commonly used GSIs block Notch signaling by inhibiting

the proteolytic activity of the γ-secretase multi-protein complex, which cleave Notch receptors at the S3 site within the transmembrane domain. In contrast to GSIs, CB-103 evidently inhibits the pathway at the most downstream level – the Notch transcriptional complex – based on its ability to block GSI-insensitive dominant active forms of NICD. Further evidence comes from the generation of a T-ALL cell line that is resistant to CB-103. The rationale of this experimental design was that drug insensitivity can be afforded through mutations, that circumvent the inhibitory activity by the drug, mutations that have the potential to reveal mechanistic insights both into the actions of the drug and its target(34). In the past this approach has been used successfully to identify drug targets for BI 2536, a Polo-like kinase1 inhibitor(50), as well as for the proteasome inhibitor Bortezomib, which is clinically used to treat multiple myeloma and mantle cell lymphoma(34, 57). Using transcriptome sequencing analysis, we identified a G193R mutation within the *RBPJ* gene, which encodes an essential component of the Notch transcription complex; this mutation confers resistance to CB-103 when introduced into Notch-driven T-ALL cells (Fig. 2). Notably, this mutant abrogated the ability of CB-103 to inhibit the formation of Notch transcription complexes, as assessed by immunoprecipitation and ChIP on endogenous Notch-response sites near target genes such as *HES1*, *DTX1*, and *MYC* (Fig. 3). In addition, computational docking studies identified the BTD domain of RBPJ as potential binding pocket for CB-103, and accurately predicted amino acids residues in RBPJ that when mutated confer resistance to CB-103. Taken together, the computational docking studies, mutational analysis as well as pulldown and ChIP experiments are in agreement with CB-103 acting as a direct inhibitor within the Notch transcription complex.

Oncogenic Notch signaling can be triggered by a variety of mutations, including single nucleotide substitutions, small insertion/deletion mutations, and rearrangements of Notch genes. One advantage of CB-103 over currently available Notch inhibitors is that it is

active against tumor cells bearing any of these types of mutations, which is not uniformly true of other Notch inhibitors. Mutated Notch receptors found in tumors with Notch gene rearrangements lack ectodomains and therefore do not rely on ligand for activation and cannot be targeted with blocking antibodies. Furthermore, approximately 5% of TNBCs and 52% of glomus tumors have gene rearrangements in *NOTCH2*(7, 8, 58) in which N2-ICD nuclear access is not gamma-secretase dependent, as translational initiation in the aberrant NOTCH2 transcripts lies C-terminal of the S3 cleavage site(7). We performed proof-of-concept experiments (Fig. 5 and *SI Appendix,* Fig. S14) using either engineered human T-ALL cell lines expressing N1-ICD and the TNBC cell line HCC1187, which has a *NOTCH2* gene rearrangement. Notably, CB-103 inhibited growth of both cell lines *in vitro* as well as the growth of HCC1187 xenotransplants, whereas GSIs were inactive.

Previous studies also identified compounds - SAHM1, IMR-1 and RIN1 - that were claimed to target the Notch transcription complex(29–31). However, in reassessing the activity of SAHM1, we were unable to confirm any "on-Notch" inhibitory effects in reporter gene assays or T-ALL cells (*SI Appendix,* Fig. S7). IMR-1 is a small chemical compound that was identified based on the strategy of inhibiting MAML1 recruitment to the Notch transcription complex(30). A side by side comparison of CB-103, the GSI LY3039478, SAHM1 and IMR-1 for their ability to block growth of a Notch-driven human T-ALL cell line showed that IMR-1 had no effect on Notch target gene expression or cell growth at doses up to 10 μM, whereas CB-103 and GSI were active (*SI Appendix,* Fig. S7). IMR-1 evidently can inhibit Notch signaling at higher concentrations, as previously reported(30, 59, 60). RIN1 is another small molecule that was recently reported to modulate the Notch transcription complex(31). This small chemical compound was identified in a reporter-based cell culture assay aimed at identifying inhibitors of interactions between RBPJ and SHARP, which is a component of a transcriptional repressor complex that binds RBPJ in the absence of NICD.

In line with this possibility, RIN1-treated cells upregulated Notch target genes, mimicking the effects of RBPJ knockdown. The activity of RIN1 has yet to be assessed, in regard to therapeutic efficacy and intestinal toxicity(31), and comparative evaluation with CB-103 warrant future consideration.

One of the major dose limiting toxicities and hurdles to the therapeutic application of pan-Notch inhibitor has been intestinal toxicity(22, 23). Genetic studies in mice show that Notch acts as a stem and progenitor cell gate keeper and is important for secretory versus absorptive cell fate differentiation. Conditional, gut-specific inactivation of *Notch1* and *2*, the ligands *Dll1* and *Dll4*, and *RBPJ* each results in the loss of proliferative crypt progenitors and conversion into post-mitotic goblet cells(40, 41, 47). A similar phenotype has been observed in mice with simultaneous gut-specific inactivation of the Notch target genes *Hes1*, *Hes3* and *Hes5*, indicating Notch signaling regulates intestinal homeostasis at least in part though *Hes* genes(49). Conversely, transgenic Notch gain-of-function experiments cause a reciprocal phenotype consisting of a block in secretory cell differentiation and an expansion of immature crypt progenitors(61). The gut phenotype created by knockout of Notch pathway components is also observed in rodents treated with potent GSIs such as dibenzazepine(47), suggesting that the gut toxicity caused by GSI is mostly driven by Notch inhibition(16). In this context it is interesting to note, that four different γ-secretase complexes exist and that most available GSI block all complexes, which is likely to account for the intestinal toxicities in GSI-treated animals or patients. A recent report showed that selective pharmacological inhibition of one (presenilin-1) of the four (PSEN) γ-secretase subclasses, is effective in reducing the leukemic burden of PSEN-1 expressing T-ALL cells in xenotransplantation assays without causing intestinal toxicity(62). Thus, selective inhibition of γ-secretase complex might be a potential therapeutic strategy for safely targeting Notch-driven tumors, provided Notch cleavage is mostly mediated by specific PSEN subclasses.

These effects of GSI involve alterations in the TF Atoh1 (also known as Math1), which is a master regulator of the secretory lineage(50, 63). Conditional gut-specific inactivation of *Atoh1* results in loss of all secretory cells and in the context of GSI-mediated Notch inhibition has been shown to be essential for goblet cell fate conversion(63).

Unexpectedly, *in vivo* administration of CB-103 to mice did not lead to the anticipated goblet cell metaplasia phenotype, which was observed in GSI-treated animals. Direct Notch target genes such as *Olmf4* and *Hes1* were both downregulated by CB-103 and GSI, indicating that CB-103 reached the target tissue. By contrast, *Atoh1* transcripts were significantly higher in GSI treated animals (Fig. 4). This distinction was confirmed in intestinal organoid cultures, excluding the possibility this result is a consequence of variation in absorption or pharmacokinetic properties *in vivo*. LY3039478-treated organoids displayed a very different morphology than CB-103-treated cultures, showing increased goblet cell differentiation and decreased proliferation compared to vehicle- or CB-103-treated organoids (*SI Appendix,* Fig. S13). The mechanisms underlying this distinction are currently unknown. Several possibilities can be considered. First, CB-103 is likely to inhibit protein-protein interaction and might therefore produce more incomplete Notch inhibition than a potent GSI. A second possibility, which is not mutually exclusive, is that CB-103 may inhibit only a subset of RBPJ complexes, leading to variation in the responsiveness of different Notch target genes. Nevertheless, in Notch-driven tumors, where the levels of signaling are well above that of normal tissues due to activating mutations, CB-103 is evidently potent enough to produce responses in preclinical models. Further work is necessary to parse out these distinctions.

In summary, our discovery and characterization of CB-103 makes a compelling case that small molecule inhibitors can be developed and used to block TF complexes, which are downstream of many aberrant signaling cascades, but have been historically intransigent to

therapeutic targeting. CB-103 interferes with the Notch TF complex, and may thereby convey a more favorable therapeutic window than previous Notch-targeting agents. Motivated by this knowledge and by its pharmacological characteristics, CB-103 is currently being evaluated in phase I/II clinical trials (https://clinicaltrials.gov/ct2/show/NCT03422679).

Materials and Methods

Details are provided in *SI Appendix* including sources of constructs, compounds, cell lines and cell culture conditions (*ex vivo*, *in vitro*), luciferase reporter assay, assays of cell cycle, proliferation, cell viability, stable transformants, and animal studies. Details of microscopy, image processing and analysis, FACS and computational docking studies are described in *SI Appendix*. Methods for Western blot, IP and ChIP, qRT-PCR, *in situ* hybridization, histology and immunostaining, RNA-seq and SLAM-seq, bioinformatic and statistical analyses are also provided in *SI Appendix.*

Data availability statement

All data generated in this study are included in the paper and *SI Appendix*.

Acknowledgements

This work was in part supported by the Swiss National Science Foundation and the Swiss Cancer League, the NCCR chemical Biology (to F.R.), the foundation “Kind und Krebs”, the “Krebsliga Zurich”, the Swiss National Science Foundation (310030-133108) and the clinical research focus program “Human Hemato-Lymphatic Diseases“ of the University of Zürich. J.C.A. is supported by Harvard University Ludwig Institute. We thank the team of the

Biomolecular Screening Facility, EPFL, Gerardo Turcatti, Marc Chambon, Nathalie Ballanfat and Manuel Bueno. We thank Viktoria Reinmüller and Jieping Zhu for compound synthesis, We thank Daniel Hall and Rhett Kovall for technical support and discussion of the mode of action of CB-103, Douglas Hanahan, and Maximilien Murone for critical reading, discussions and editing of the manuscript. Molecular graphics and analyses were performed with UCSF Chimera, University of California, San Francisco, (NIH P41-GM103311).

Conflict of interest

The authors declare competing financial interests. R.L. and F.R. are cofounders and R.L., M.V. and C.U. are employees of Cellestia Biotech AG.

References

1. C. Siebel, U. Lendahl, Notch Signaling in Development, Tissue Homeostasis, and Disease. *Physiol. Rev.* **97**, 1235–1294 (2017).

2. R. Kopan, Ma. X. G. Ilagan, The Canonical Notch Signaling Pathway: Unfolding the Activation Mechanism. *Cell* **137**, 216–233 (2009).

3. A. P. Weng, *et al.*, Activating Mutations of NOTCH1 in Human T Cell Acute Lymphoblastic Leukemia. *Science* **306**, 269–271 (2004).

4. R. Kridel, *et al.*, Whole transcriptome sequencing reveals recurrent NOTCH1 mutations in mantle cell lymphoma. *Blood* **119**, 1963–1971 (2012).

5. E. Rosati, *et al.*, NOTCH1 Aberrations in Chronic Lymphocytic Leukemia. *Front. Oncol.* **8** (2018).

6. R. Ferrarotto, *et al.*, Activating NOTCH1 Mutations Define a Distinct Subgroup of Patients With Adenoid Cystic Carcinoma Who Have Poor Prognosis, Propensity to Bone and Liver Metastasis, and Potential Responsiveness to Notch1 Inhibitors. *J. Clin. Oncol. Off. J. Am. Soc. Clin. Oncol.* **35**, 352–360 (2017).

7. D. R. Robinson, *et al.*, Functionally recurrent rearrangements of the MAST kinase and Notch gene families in breast cancer. *Nat. Med.* **17**, 1646–1651 (2011).

8. A. Stoeck, *et al.*, Discovery of Biomarkers Predictive of GSI Response in Triple-Negative Breast Cancer and Adenoid Cystic Carcinoma. *Cancer Discov.* **4**, 1154–1167 (2014).

9. J. Ridgway, *et al.*, Inhibition of Dll4 signalling inhibits tumour growth by deregulating angiogenesis. *Nature* **444**, 1083–1087 (2006).

10. I. Noguera-Troise, *et al.*, Blockade of Dll4 inhibits tumour growth by promoting non-productive angiogenesis. *Nature* **444**, 1032–1037 (2006).

11. J.-L. Li, *et al.*, Delta-like 4 Notch Ligand Regulates Tumor Angiogenesis, Improves Tumor Vascular Function, and Promotes Tumor Growth In vivo. *Cancer Res.* **67**, 11244–11253 (2007).

12. Y. Wu, *et al.*, Therapeutic antibody targeting of individual Notch receptors. *Nature* **464**, 1052–1057 (2010).

13. K. Li, *et al.*, Modulation of Notch Signaling by Antibodies Specific for the Extracellular Negative Regulatory Region of NOTCH3. *J. Biol. Chem.* **283**, 8046–8054 (2008).

14. E. R. Andersson, U. Lendahl, Therapeutic modulation of Notch signalling — are we there yet? *Nat. Rev. Drug Discov.* **13**, 357–378 (2014).

15. Y. Ran, *et al.*, γ-Secretase inhibitors in cancer clinical trials are pharmacologically and functionally distinct. *EMBO Mol. Med.* **9**, 950–966 (2017).

16. A. Haapasalo, D. M. Kovacs, The Many Substrates of Presenilin/γ-Secretase. *J. Alzheimers Dis.* **25**, 3–28 (2011).

17. W.-C. Yen, *et al.*, Targeting Notch Signaling with a Notch2/Notch3 Antagonist (Tarextumab) Inhibits Tumor Growth and Decreases Tumor-Initiating Cell Frequency. *Clin. Cancer Res.* **21**, 2084–2095 (2015).

18. S. Minuzzo, *et al.*, DLL4 regulates NOTCH signaling and growth of T acute lymphoblastic leukemia cells in NOD/SCID mice. *Carcinogenesis* **36**, 115–121 (2015).

19. J. Han, Q. Shen, Targeting γ-secretase in breast cancer. *Breast Cancer Targets Ther.* (2012) https:/doi.org/10.2147/BCTT.S26437 (October 4, 2019).

20. B. Knoechel, *et al.*, Complete hematologic response of early T-cell progenitor acute lymphoblastic leukemia to the γ-secretase inhibitor BMS-906024: genetic and epigenetic findings in an outlier case. *Mol. Case Stud.* **1**, a000539 (2015).

21. C. Papayannidis, *et al.*, A Phase 1 study of the novel gamma-secretase inhibitor PF-03084014 in patients with T-cell acute lymphoblastic leukemia and T-cell lymphoblastic lymphoma. *Blood Cancer J.* **5**, e350–e350 (2015).

22. D. C. Smith, *et al.*, A phase 1 dose escalation and expansion study of Tarextumab (OMP-59R5) in patients with solid tumors. *Invest. New Drugs* **37**, 722–730 (2019).

23. Z. I. Hu, *et al.*, A randomized phase II trial of nab-paclitaxel and gemcitabine with tarextumab or placebo in patients with untreated metastatic pancreatic cancer. *Cancer Med.* **8**, 5148–5157 (2019).

24. C. Massard, *et al.*, First-in-human study of LY3039478, an oral Notch signaling inhibitor in advanced or metastatic cancer. *Ann. Oncol.* **29**, 1911–1917 (2018).

25. K. L. Aung, *et al.*, A multi-arm phase I dose escalating study of an oral NOTCH inhibitor BMS-986115 in patients with advanced solid tumours. *Invest. New Drugs* **36**, 1026–1036 (2018).

26. Y. Nam, P. Sliz, L. Song, J. C. Aster, S. C. Blacklow, Structural Basis for Cooperativity in Recruitment of MAML Coactivators to Notch Transcription Complexes. *Cell* **124**, 973–983 (2006).

27. Y. Nam, A. P. Weng, J. C. Aster, S. C. Blacklow, Structural Requirements for Assembly of the CSL·Intracellular Notch1·Mastermind-like 1 Transcriptional Activation Complex. *J. Biol. Chem.* **278**, 21232–21239 (2003).

28. I. Maillard, Mastermind critically regulates Notch-mediated lymphoid cell fate decisions. *Blood* **104**, 1696–1702 (2004).

29. R. E. Moellering, *et al.*, Direct inhibition of the NOTCH transcription factor complex. *Nature* **462**, 182–188 (2009).

30. L. Astudillo, *et al.*, The Small Molecule IMR-1 Inhibits the Notch Transcriptional Activation Complex to Suppress Tumorigenesis. *Cancer Res.* **76**, 3593–3603 (2016).

31. C. Hurtado, *et al.*, Disruption of NOTCH signaling by a small molecule inhibitor of the transcription factor RBPJ. *Sci. Rep.* **9**, 1–9 (2019).

32. D. Herranz, *et al.*, A NOTCH1-driven *MYC* enhancer promotes T cell development, transformation and acute lymphoblastic leukemia. *Nat. Med.* **20**, 1130–1137 (2014).

33. Y. Yashiro-Ohtani, *et al.*, Long-range enhancer activity determines Myc sensitivity to Notch inhibitors in T cell leukemia. *Proc. Natl. Acad. Sci.* **111**, E4946–E4953 (2014).

34. S. A. Wacker, B. R. Houghtaling, O. Elemento, T. M. Kapoor, Using transcriptome sequencing to identify mechanisms of drug action and resistance. *Nat. Chem. Biol.* **8**, 235–237 (2012).

35. D. R. Armstrong, *et al.*, PDBe: improved findability of macromolecular structure data in the PDB. *Nucleic Acids Res.* **48**, D335–D343 (2020).

36. H. Wang, *et al.*, NOTCH1–RBPJ complexes drive target gene expression through dynamic interactions with superenhancers. *Proc. Natl. Acad. Sci.* **111**, 705–710 (2014).

37. H. Liu, *et al.*, Notch dimerization is required for leukemogenesis and T-cell development. *Genes Dev.* **24**, 2395–2407 (2010).

38. K. L. Arnett, *et al.*, Structural and mechanistic insights into cooperative assembly of dimeric Notch transcription complexes. *Nat. Struct. Mol. Biol.* **17**, 1312–1317 (2010).

39. F. Schweisguth, J. W. Posakony, Suppressor of Hairless, the Drosophila homolog of the mouse recombination signal-binding protein gene, controls sensory organ cell fates. *Cell* **69**, 1199–1212 (1992).

40. O. Riccio, *et al.*, Loss of intestinal crypt progenitor cells owing to inactivation of both Notch1 and Notch2 is accompanied by derepression of CDK inhibitors p27Kip1 and p57Kip2. *EMBO Rep.* **9**, 377–383 (2008).

41. L. Pellegrinet, *et al.*, Dll1- and Dll4-Mediated Notch Signaling Are Required for Homeostasis of Intestinal Stem Cells. *Gastroenterology* **140**, 1230-1240.e7 (2011).

42. T. Saito, *et al.*, Notch2 Is Preferentially Expressed in Mature B Cells and Indispensable for Marginal Zone B Lineage Development. *Immunity* **18**, 675–685 (2003).

43. K. Hozumi, *et al.*, Delta-like 1 is necessary for the generation of marginal zone B cells but not T cells *in vivo*. *Nat. Immunol.* **5**, 638–644 (2004).

44. F. Radtke, *et al.*, Deficient T Cell Fate Specification in Mice with an Induced Inactivation of Notch1. *Immunity* **10**, 547–558 (1999).

45. K. L. Lewis, *et al.*, Notch2 Receptor Signaling Controls Functional Differentiation of Dendritic Cells in the Spleen and Intestine. *Immunity* **35**, 780–791 (2011).

46. M. Ehling, S. Adams, R. Benedito, R. H. Adams, Notch controls retinal blood vessel maturation and quiescence. *Development* **140**, 3051–3061 (2013).

47. J. H. van Es, *et al.*, Notch/γ-secretase inhibition turns proliferative cells in intestinal crypts and adenomas into goblet cells. *Nature* **435**, 959–963 (2005).

48. K. L. VanDussen, *et al.*, Notch signaling modulates proliferation and differentiation of intestinal crypt base columnar stem cells. *Development* **139**, 488–497 (2012).

49. T. Ueo, *et al.*, The role of Hes genes in intestinal development, homeostasis and tumor formation. *Development* **139**, 1071–1082 (2012).

50. Q. Yang, N. A. Bermingham, M. J. Finegold, H. Y. Zoghbi, Requirement of Math1 for Secretory Cell Lineage Commitment in the Mouse Intestine. *Science* **294**, 2155–2158 (2001).

51. M. Sanchez-Martin, A. Ferrando, The NOTCH1-MYC highway towards T-cell acute lymphoblastic leukemia. *Blood*, blood-2016-09-692582 (2017).

52. B. Cohen, *et al.*, Cyclin D1 is a direct target of JAG1-mediated Notch signaling in breast cancer. *Breast Cancer Res. Treat.* **123**, 113–124 (2010).

53. L. Li, *et al.*, Notch-1 Signaling Promotes the Malignant Features of Human Breast Cancer through NF-κB Activation. *PLOS ONE* **9**, e95912 (2014).

54. Q. Wang, *et al.*, Elevating H3K27me3 level sensitizes colorectal cancer to oxaliplatin. *J. Mol. Cell Biol.* https:/doi.org/10.1093/jmcb/mjz032 (December 19, 2019).

55. M. J. Kiel, *et al.*, Whole-genome sequencing identifies recurrent somatic NOTCH2 mutations in splenic marginal zone lymphoma. *J. Exp. Med.* **209**, 1553–1565 (2012).

56. J. C. Aster, W. S. Pear, S. C. Blacklow, The Varied Roles of Notch in Cancer. *Annu. Rev. Pathol. Mech. Dis.* **12**, 245–275 (2017).

57. D. Chen, M. Frezza, S. Schmitt, J. K. and Q. P. Dou, Bortezomib as the First Proteasome Inhibitor Anticancer Drug: Current Status and Future Perspectives. *Curr. Cancer Drug Targets* (2011) (October 18, 2019).

58. J.-M. Mosquera, *et al.*, Novel MIR143-NOTCH fusions in benign and malignant glomus tumors. *Genes. Chromosomes Cancer* **52**, 1075–1087 (2013).

59. H. Zhou, *et al.*, Paeonol reverses promoting effect of the HOTAIR/miR-124/Notch1 axis on renal interstitial fibrosis in a rat model. *J. Cell. Physiol.* **234**, 14351–14363 (2019).

60. Z. Zhang, S. Zhao, D. Lian, D. He, L. Li, Notch1 signalling pathway promotes proliferation and mediates differentiation direction in hippocampus of Streptococcus pneumonia meningitis rats. *J. Infect. Dis.*, jiz414 (2019).

61. S. Fre, *et al.*, Notch signals control the fate of immature progenitor cells in the intestine. *Nature* **435**, 964–968 (2005).

62. R. A. Habets, *et al.*, Safe targeting of T cell acute lymphoblastic leukemia by pathology-specific NOTCH inhibition. *Sci. Transl. Med.* **11** (2019).

63. J. H. van Es, N. de Geest, M. van de Born, H. Clevers, B. A. Hassan, Intestinal stem cells lacking the Math1 tumour suppressor are refractory to Notch inhibitors. *Nat. Commun.* **1**, 18 (2010).

64. S. H. Choi, *et al.*, Conformational Locking upon Cooperative Assembly of Notch Transcription Complexes. *Structure* **20**, 340–349 (2012).

Figure legends

Fig. 1. Identification of CB-103 as a novel inhibitor of the Notch transcription activation complex. (A) Schematic of the Delta-like 4 (DL4) Notch1 (N1) co-culture assay used high-throughput screening in HeLa cells. Ligand-receptor mediated pathway activation was measured using a Notch responsive luciferase reporter. (B) Assay validation of the DL4-N1 co-culture screening with indicated Z' value. Bar graph shows result of one representative 384-well plate, half treated with 10 μM of the GSI DAPT and half with vehicle control. (C) Schematic representation of the N1-ICD-driven luciferase reporter assay used to counter screen validated hits of the primary screen. (D) Chemical structure of 6-(4-(*tert*-butyl)phenoxy)pyridine-3-amine (CB-103). (E) Bar graphs show concentration dependent

assessment of CB-103 and GSI (DAPT) to DL4-Notch1-mediated signaling in the RBPJ-driven reporter and co-culture assay. Luciferase activity was measured 24 hours after treatment. (F) Dose-response curves for mNotch1, mNotch2, mNotch3 and mNotch4 activation following treatment of co-cultures with CB-103. (G) Bar graph shows concentration dependent assessment of CB-103 and GSI (DAPT) to inhibit N1-ICD-mediated, RBPJ-driven reporter assay. (H) Dose-response curves for N1-ICD, N2-ICD, N3-ICD N4-ICD mediated RBPJ luciferase reporter assay 24 hours post CB-103 treatment. (I) Nuclear localization of N1-ICD-GFP fusion protein in HeLa cells in the presence of DMSO or CB-103 (representative of 3 independent experiments). (J) N1-ICD-induced luciferase activity in the presence of CB-103 and increasing amounts of MAML1.

Fig. 2. Single amino acid mutations within the BTD domain of RBPJ cause unresponsiveness to CB-103 in RPMI-8402 cells. (A) Experimental structure of the NOTCH1 transcription complex on the HES1 promoter DNA sequence (PDB ID 3V79) (64). CSL (orange), domains are show in ribbon representation. HES1 backbone is shown in ribbon representation, with nucleotides displayed as tubes. Green arrows indicate predicted amino acids important for binding of CB-103 within the BTD domain of RBPJ. (B) Graph shows dose response curves of CB-103 treated parental, RPBJ^{wt}–V5 and RBPJ^{G193R}–V5, RBPJ^{L245A}–V5, RBPJ^{L248A}–V5, RBPJ^{F196A}–V5 and RBPJ^{G194R}–V5 expressing RPMI-8402 cells. Cells were treated with CB-103 for 3 days. IC-50 values for respective cell lines are indicated. (C) Bar graphs show percentage of apoptotic cells of parental, RBPJ^{wt}–V5 and RBPJ^{G193R}–V5, RBPJ^{L245A}–V5, RBPJ^{L248A}–V5, RBPJ^{F196A}–V5 and RBPJ^{G194R}–V5 expressing RPMI-8402 cells treated with DMSO or CB-103 (10 μM) for 72 hours. Statistical analysis was performed using two-tailed t-test (*** $p < 0.0005$, **$p<0.007$).

Fig. 3. CB-103 inhibits assembly of the RBPJ-NICD transcription complex. (A and B) RPMI-8402 cells expressing either $RBPJ^{wt}$-V5 (A) or $RBPJ^{G193R}$-V5 mutant protein (B), were treated with vehicle control (-) or CB-103 (+), 10 μM for 14 hours and subjected to immunoprecipitation using a V5-specific antibody. N1-ICD immunoprecipitates were assessed by Western blot. Western blot analysis for MYC expression was performed on input: parental, $RBPJ^{wt}$-V5 or $RBPJ^{G193R}$-V5 mutant protein expressing RPMI-8402 cells. (C) DMSO- or CB-103-treated RPMI-8402 cells expressing either $RBPJ^{wt}$-V5 or $RBPJ^{G193R}$-V5 protein were subjected to ChIP. RBPJ binding regions from NOTCH target genes *HES1*, *DTX1* and *MYC* were PCR amplified from input and precipitated DNA. Location of the PCR amplicons is schematically illustrated to the left (red dash). Results are expressed as percentage relative to input. Shown are mean ± SD ($n \geq 3$). Statistical analysis was performed using one-way ANOVA (**** $p < 0.0001$, *** $p < 0.0006$, ** $p < 0.009$).

Fig. 4. CB-103 reduces *Notch* target gene expression in the small intestine without causing goblet cell metaplasia. (A) Alcian blue (top panels), Ki67 staining (lower panels) and *in situ* hybridizations for expression of *Notch* target genes *Olmf4*, *Hes1* and *Atoh1* of representative sections from the proximal small intestine of vehicle, CB-103 (20 mg/kg/ 2 x day) and GSI (LY3039478, 20 mg/kg/ 2 x day) treated mice are shown. Mice were treated with CB-103 up to 4 weeks and analyzed at either 1- or 4-weeks post administration. Analysis at two time points revealed comparable results. CB-103 treatment at 4 weeks and GSI treatment at 1 week is depicted. (B) Bar graphs show quantification of indicated stainings and *in situ* hybridizations. The number of Alcian blue positive cells per crypt-villus unit and Ki67 positive cells per crypt is expressed as percentage of positive cells per field, of vehicle (n=2

mice, 130 crypt-villus units for Alcian blue and 462 crypts for Ki67), CB-103 (n=6 mice, 375 crypt-villus units and 430 crypts for Ki67) and GSI (n=3 mice, 135 crypt villus-units and 330 crypts for Ki67) treated animals. *In situ* hybridization of *Olmf4*, *Hes1* and *Atoh1* expression was quantified and is expressed as percentage of positive crypts for *Olmf4* (score 4, n=2 mice for vehicle treated animals, 190 crypts, n=6 mice for CB-103 treatment, 600 crypts, n=3 mice for GSI-treated animals, 300 crypts,), percentage of positive cells per crypt for *Hes1*(score 4, n=2 mice for vehicle treated animals, 140 crypts, n=6 mice for CB-103 treatment, 170 crypts, n=3 mice for GSI-treated animals, 110 crypts) and percentage of positive cells per field for *Atoh1* expression (n=2 mice, vehicle group, 150 crypt-villus units, n=6 mice, CB-103 group, 340 crypt-villus units, n=3 mice, LY3039478 group, 220 crypt-villus units). Scale bar for Alcian blue = 50μm, for other slides = 20μm. Statistical analysis was performed using unpaired t-test. (**** $p < 0.0001$).

Fig. 5 CB-103 impedes growth of NOTCH-positive cancer cell lines and primary human T-ALL. (A). Growth kinetics of HCC-1187 cells treated with DMSO, GSI (RO4929097) and CB-103 (10μM each) for 6 days. (B) Luciferase-expressing HCC-1187 cells were subcutaneously transplanted into NOD/SCIDγc$^{-/-}$ (NSG) mice and treated with either vehicle (n=6) or CB-103 (n=6) for 15d (2x/day). Bioluminescence was measured 30 days post transplantation. HCC-1187 tumor volume (mm^3) measured over time in xenotransplanted mice treated with either vehicle or CB-103 (25mg/kg) administrated twice a day (n=6 for each group) is shown. Two independent experiments were performed. Statistical analysis was performed using two-way ANOVA **** $p < 0.00001$. (C) Representative hematoxylin and eosin (H&E) staining (left panel) and immunostaining for Cyclin D1 (right panel) of tumors harvested from vehicle and CB-103 treated animals is shown. (D) Oxaliplatin-resistant M43 colorectal cancer cells were transplanted into NSG mice and subsequently treated with either

vehicle (n=18), CB-103 (n=18), oxaliplatin, or oxaliplatin and CB-103 for 12 days (25 mg/kg 1x/day) and tumor growth fold-change was monitored over time (left panel) and at end stage of the experiment (right panel). One-way ANOVA, Tukey's multiple comparisons test * $p < 0.05$; *** $p < 0.0003$; **** $p < 0.0001$. (E) Response to CB-103 of T-ALL cells *in vitro*. Patient derived xenografts (n=20) were maintained on human mesenchymal stromal cells and incubated with 0.01, 0.1, 1, 10 or 25 μM CB-103 for 7 days. Graph represents IC_{50} values of each patient sample treated with CB-103. Blue circles = patient samples positive for the presence N1-ICD, red circles = patient samples negative for N1-ICD. (F) Immunoblots underneath show N1-ICD levels decrease upon treatment with CB-103. N1-ICD detection in indicated patient samples (numbered) on Western blot after 72 hours exposure to DMSO or CB-103 is shown. Mutation status for *NOTCH1* and *FBXW7* are indicated. (G) Event-free survival analysis after treatment of leukemia xenografts of the T-ALL corresponding to case 1. Kaplan-Meier survival curve is shown for xenografted NSG mice. Treatment with vehicle or CB-103 as indicated when 10% of T-ALL cells were detected in peripheral blood by flow cytometry. Log-rank (Mantel-Cox) test and p-value as indicated. Bar graph represents detection levels of N1-ICD in T-ALL cells after *in vivo* treatment with CB-103. The mean ratio (+/- SEM) of N1-ICD (Val 1744) determined in vehicle and CB-103 treated animals (two per condition). A representative Western blot example for N1-ICD of treated animals is shown. (H) Bar graphs show results of a second independent N1-ICD positive PDX model xenografted into NSG mice. Vehicle control and CB-103 treatment groups were subdivided into high and low tumor burden groups based on >20% and <2% of T-ALL cells detected in peripheral blood by flow cytometric analysis at treatment initiation. Animals groups were treated for 12 days with either vehicle control or CB-103. Bar graphs show absolute numbers of $huCD45^{+}CD7^{+}$ T-ALL cells after treatment. Animals with high tumor burden: n=5 for

vehicle control and n=3 for CB-103 treated animals; animals with low tumor burden: n=5 for both vehicle and CB-103 treated animals. Statistical analysis: Students t-test test * $p < 0.05$.

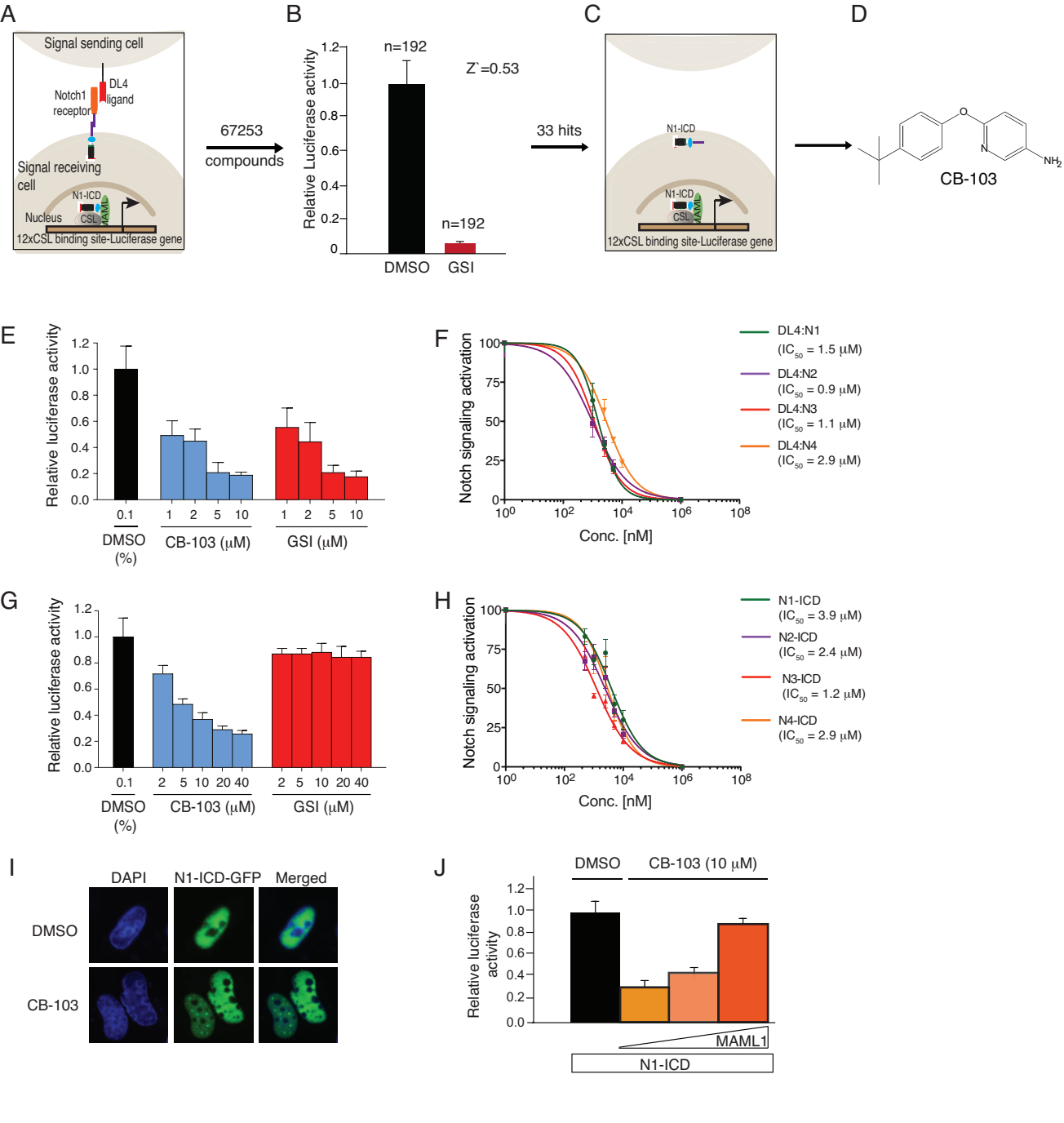
A
Signal sending cell
Notch1 receptor
DL4 ligand
Signal receiving cell
N1-ICD
CSL
MAML
Nucleus
12xCSL binding site-Luciferase gene
67253 compounds
B
Relative Luciferase activity
n=192
n=192
Z`=0.53
DMSO
GSI
33 hits
C
N1-ICD
12xCSL binding site-Luciferase gene
D
CB-103
E
Relative luciferase activity
DMSO (%)
CB-103 (μM)
GSI (μM)
F
Notch signaling activation
Conc. [nM]
DL4:N1 (IC50 = 1.5 μM)
DL4:N2 (IC50 = 0.9 μM)
DL4:N3 (IC50 = 1.1 μM)
DL4:N4 (IC50 = 2.9 μM)
G
Relative luciferase activity
DMSO (%)
CB-103 (μM)
GSI (μM)
H
Notch signaling activation
Conc. [nM]
N1-ICD (IC50 = 3.9 μM)
N2-ICD (IC50 = 2.4 μM)
N3-ICD (IC50 = 1.2 μM)
N4-ICD (IC50 = 2.9 μM)
I
DAPI
N1-ICD-GFP
Merged
DMSO
CB-103
J
DMSO
CB-103 (10 μM)
Relative luciferase activity
MAML1
N1-ICD

Figure 1

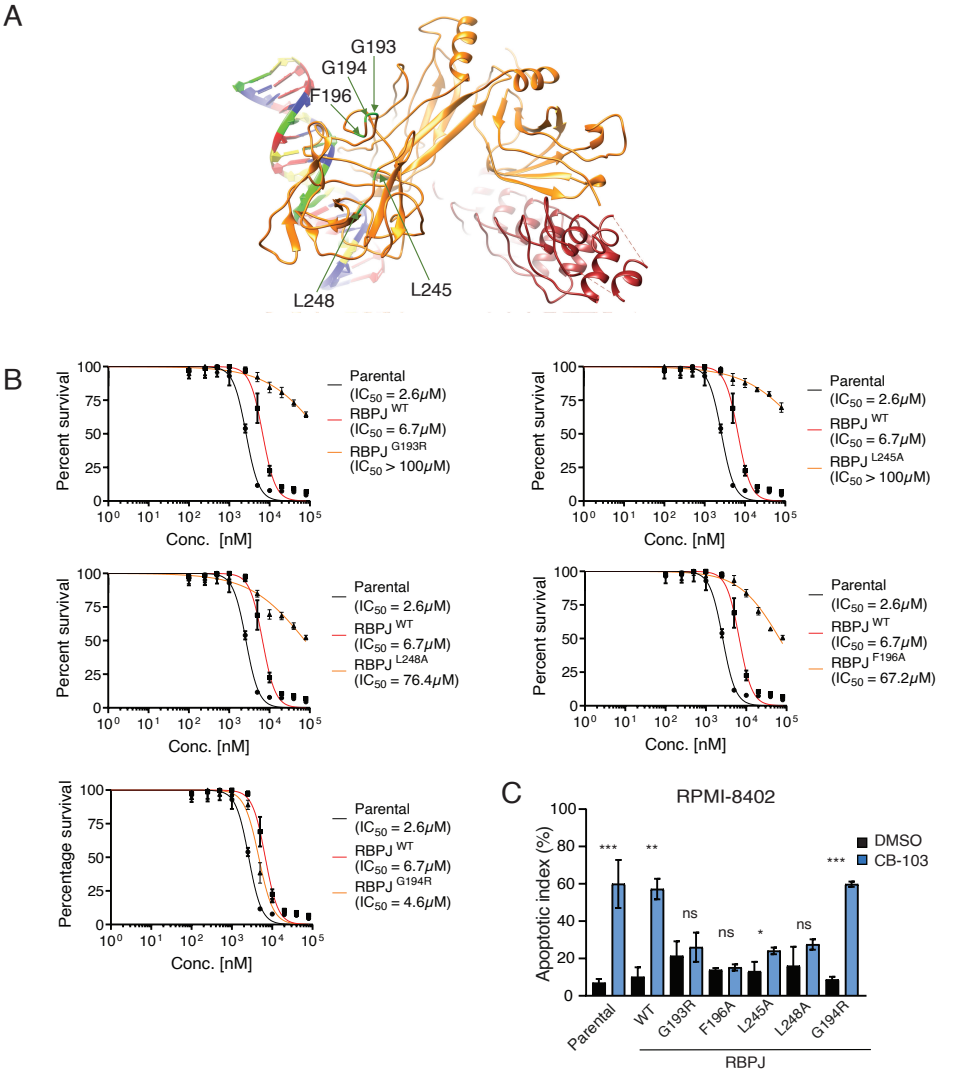
A
G193
G194
F196
L248
L245
B
Percent survival
Conc. [nM]
Parental (IC50 = 2.6μM)
RBPJ WT (IC50 = 6.7μM)
RBPJ G193R (IC50 > 100μM)
RBPJ L245A (IC50 > 100μM)
RBPJ L248A (IC50 = 76.4μM)
RBPJ F196A (IC50 = 67.2μM)
Percentage survival
RBPJ G194R (IC50 = 4.6μM)
C
RPMI-8402
Apoptotic index (%)
DMSO
CB-103
ns
Parental
WT
G193R
F196A
L245A
L248A
G194R
RBPJ

Figure 2

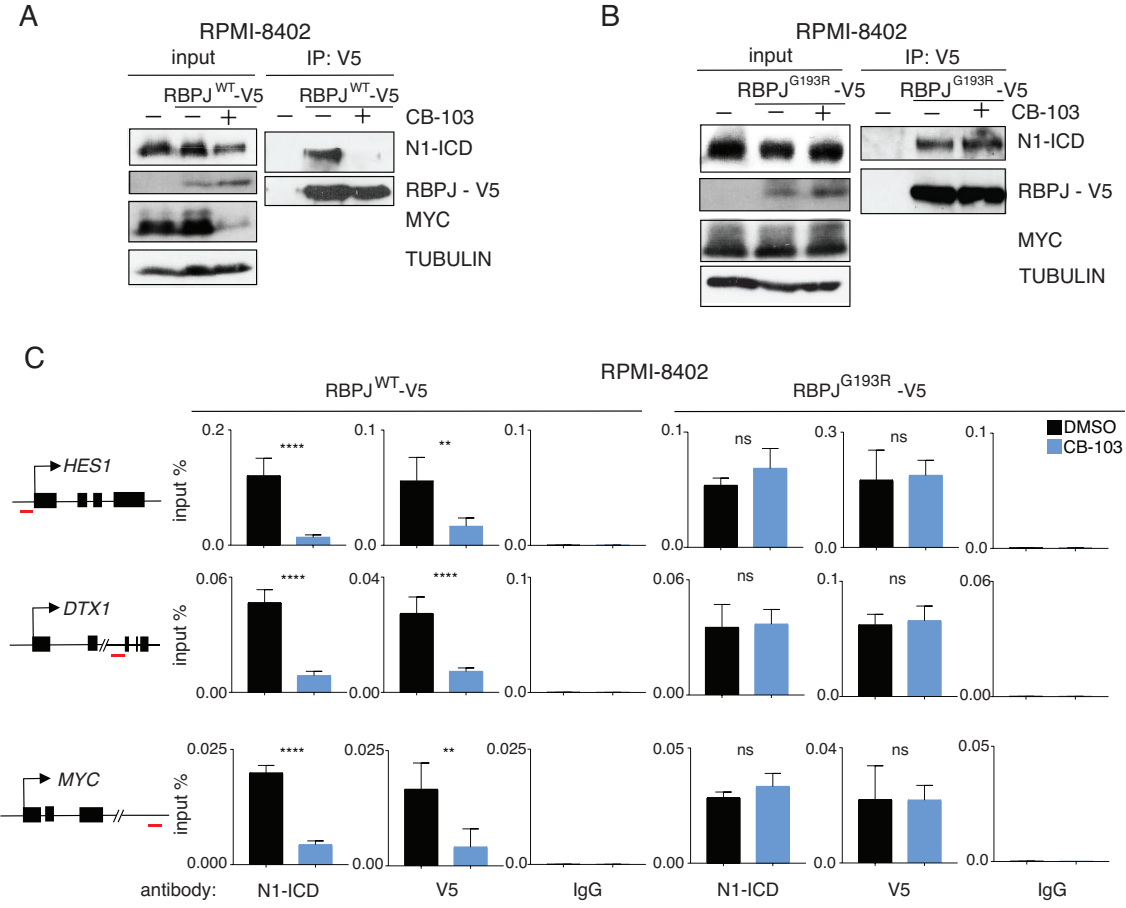
A
RPMI-8402
input
IP: V5
RBPJ WT-V5
RBPJ WT-V5
CB-103
N1-ICD
RBPJ - V5
MYC
TUBULIN
B
RPMI-8402
input
IP: V5
RBPJ G193R -V5
RBPJ G193R -V5
CB-103
N1-ICD
RBPJ - V5
MYC
TUBULIN
C
RPMI-8402
RBPJ WT-V5
RBPJ G193R -V5
DMSO
CB-103
HES1
DTX1
MYC
input %
****
**
ns
antibody:
N1-ICD
V5
IgG

Figure 3

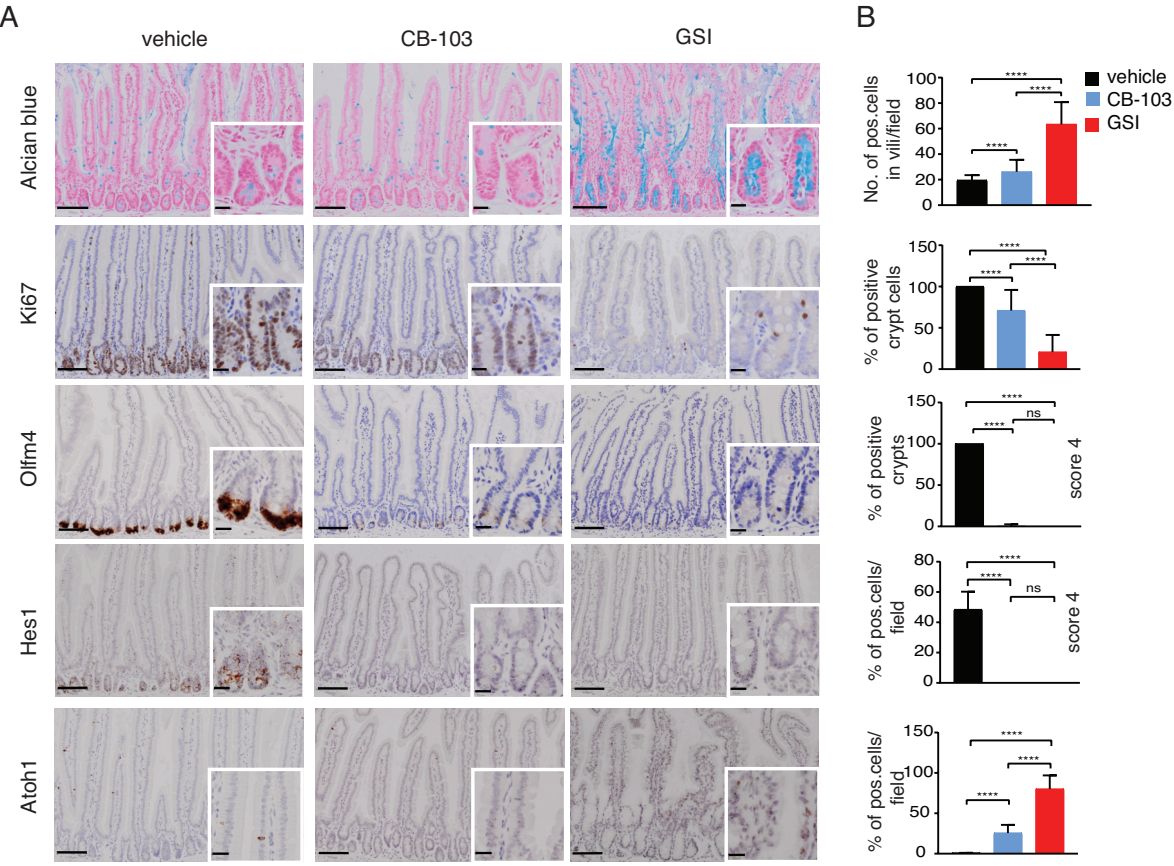
A
vehicle
CB-103
GSI
Alcian blue
Ki67
Olfm4
Hes1
Atoh1
B
vehicle
CB-103
GSI
No. of pos.cells in vili/field
% of positive crypt cells
% of positive crypts
score 4
% of pos.cells/ field
score 4
% of pos.cells/ field
****
ns

Figure 4

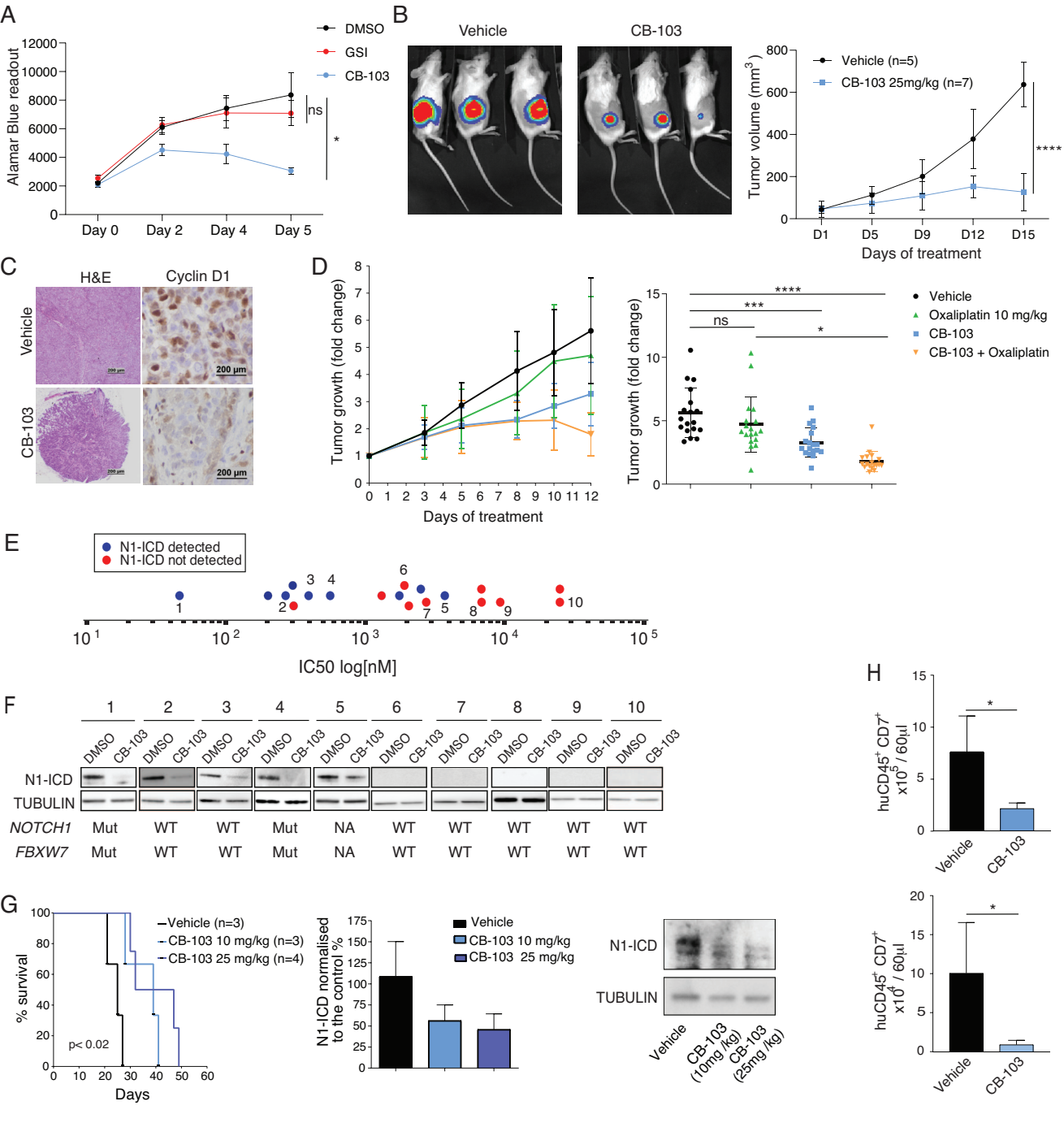
A
DMSO
GSI
CB-103
Alamar Blue readout
12000
10000
8000
6000
4000
2000
0
Day 0
Day 2
Day 4
Day 5
ns
*
B
Vehicle
CB-103
Vehicle (n=5)
CB-103 25mg/kg (n=7)
Tumor volume (mm3)
800
600
400
200
0
D1
D5
D9
D12
D15
Days of treatment
****
C
H&E
Cyclin D1
Vehicle
CB-103
200 µm
D
Tumor growth (fold change)
Days of treatment
Vehicle
Oxaliplatin 10 mg/kg
CB-103
CB-103 + Oxaliplatin
****
***
ns
*
E
N1-ICD detected
N1-ICD not detected
IC50 log[nM]
F
N1-ICD
TUBULIN
NOTCH1
FBXW7
Mut
WT
NA
G
Vehicle (n=3)
CB-103 10 mg/kg (n=3)
CB-103 25 mg/kg (n=4)
% survival
p< 0.02
Days
N1-ICD normalised to the control %
Vehicle
CB-103 10 mg/kg
CB-103 25 mg/kg
N1-ICD
TUBULIN
Vehicle
CB-103 (10mg/kg)
CB-103 (25mg/kg)
H
huCD45+ CD7+ x10^5 / 60µl
huCD45+ CD7+ x10^4 / 60µl
Vehicle
CB-103

Figure 5